Thickness and optical constants measurement of thin film growth with circular heterodyne interferometry

Cheng-Chih Hsu [a,*], Ju-Yi Lee [b], Der-Chin Su [c]

[a]*Center for Measurement Standards, Industrial Technology Research Institute, 321 Kuang Fu Rd., Sec. 2, Hsin Chu 300, Taiwan, ROC*
[b]*Department of Mechanical Engineering, National Central University, 300 Jhong Da Rd., Chung Li 320, Taiwan, ROC*
[c]*Institute of Electro-Optical Engineering, National Chiao Tung University, 1001 Ta Hsueh Rd., Hsin Chu 300, Taiwan, ROC*

Abstract

In this article, we report an alternative method for in situ monitoring of the thickness and refractive index of thin film during the growth process. We design a special structure with a thickness-controlled air film to simulate the process of thin film growth. The phase term of the reflected light coming from this multi-layer structure is modulated and has a strong correlation with the thickness and optical constant of the thin air film within this structure. Based on the phase demodulated technique and the multiple beam reflection theory under the specific oblique incident angle, the thickness and refractive index of thin film can be measured with a single configuration. According to the theoretical prediction, the resolution of the thickness determination of the thin film should be better than 0.05 nm.
© 2005 Elsevier B.V. All rights reserved.

Keywords: Optical constants; Interferometry; Thickness monitoring

1. Introduction

Thin film growth measurement for the production of high quality electronic [1–4] and optoelectronic [5–7] devices is the most important and has attracted considerable interests. One of the most recent examples in the field of thin film technology is the vertical cavity surface emitting laser (VCSEL) [5–7], which is of great importance for various applications in optical communication, optical interconnects and optical disc read-out systems [7]. The multilayers in VCSEL are difficult to grow and the required accuracy of the grown thickness must be within of ±2% [5,7], especially in Bragg reflectors. A small thickness mismatch will dramatically affect the device performance.

To certify that the accuracy of thickness under the growth process does not exceed the expected values, many measurement methods have been proposed. The common optical method for characterizing thin films is the ellipsom-etry [1–6]. In a common single ellipsometric measurement, two parameters ψ and Δ can be obtained at a single incident angle. But in this method, these parameters do not measure with truly phase detection and the unique measurement results of these parameters will be achieved with numerical curve fitting. Compared with the ellipsometry, an alternative method based on the circular heterodyne interferometry, truly phase detection, and the multiple-beam interference theory is proposed in this paper. In this method, we can obtain many different sets of data without changing the incident angle, wavelength, and numerical curve fitting process, just by changing the azimuth angles of the analyzer.

In our method, we can simultaneously estimate the refractive index and thickness of thin film with a single optical configuration. To demonstrate that this method could be applied to a real thin film growth system, we design a special configuration to simulate the behavior of the thin film growth in a real system. This configuration consists of a glass plate (BK7) and a metallic (Au) mirror with a motorized mount, and there is a small air gap between them. The forward and backward movements of the mirror simulate the thickness variations in the thin film growth or

---

etching. Because of the common-path optical configuration and the heterodyne interferometric phase measurement, this method can avoid surrounding vibration and thus achieve high stability and resolution. According to the theoretical prediction, the resolution of the thickness of the thin film is better than 0.05 nm, and this method may be useful in ultra-thin film growth monitoring.

2. Principle

Fig. 1 shows a schematic diagram of this method, in which a simulated structure takes the place of a real molecule beam epitaxy (MBE) system. This simulated
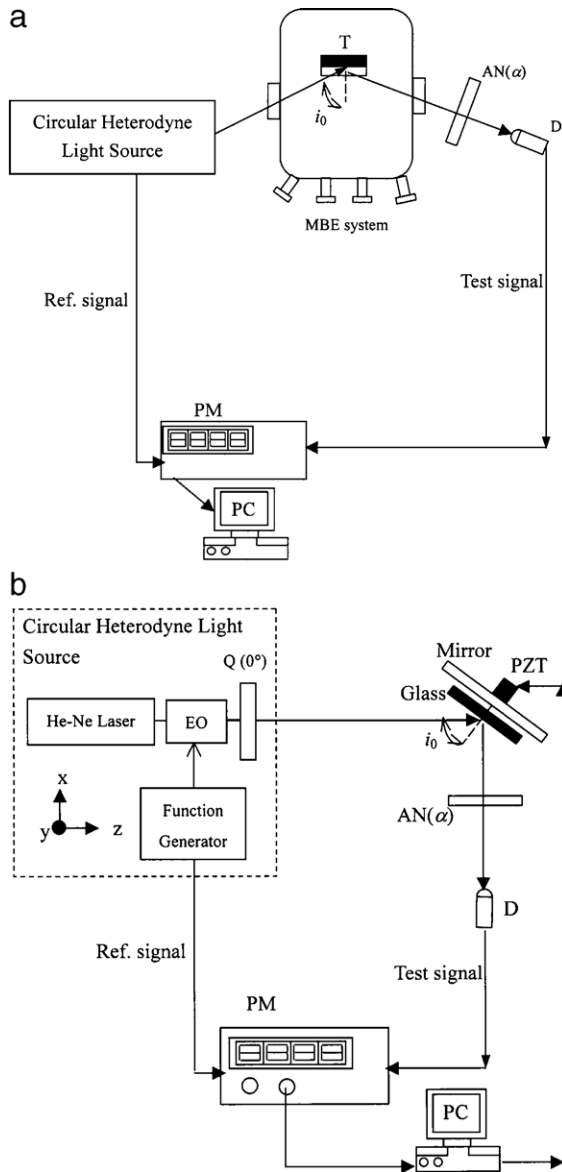

Fig. 1. Schematic diagram of this method for measuring the phase difference operated in (a) operated in real MBE system, and (b) a simulated configuration. EO: Electro-optic modulator; Q: Quarter-wave plate; D: Detector; AN: Analyzer; PM: Phase meter; T: Test medium.
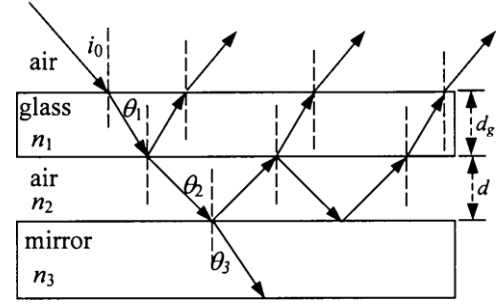

Fig. 2. Multiple-beam reflection in thin air spacing.

configuration consists of a glass (BK7) plate and a metallic (Au) mirror, and there is a thin air spacing between them (Fig. 2). The mirror is mounted on the piezo translator (PZT) that can move forward and backward to simulate the thickness variations in the thin film growth/etching. Of course, the air spacing in this structure is a substitute for the real thin film. For simplicity, the $+z$-axis is chosen to be along the light propagation direction and the y-axis is along the direction perpendicular to the paper plane. A circular heterodyne light source [8] with angular frequency difference ω between the left- and right-polarizations is used. The light beam is incident at i_0 to the test medium T, and it is multiply reflected at both sides of the thin air gap. The multiply reflected light beams pass through the analyzer (AN) with the transmission axis at α degree to the x-axis and enter the photodetector D. The total amplitudes at D can be expressed as [8]

$$E_t = AN(\alpha) \cdot S \cdot E_i$$

$$= \begin{pmatrix} \cos^2\alpha & \sin\alpha\cos\alpha \\ \sin\alpha\cos\alpha & \sin^2\alpha \end{pmatrix} \begin{pmatrix} z_p & 0 \\ 0 & z_s \end{pmatrix} \begin{pmatrix} \cos\frac{\omega t}{2} \\ -\sin\frac{\omega t}{2} \end{pmatrix}$$

$$= \begin{pmatrix} E_{tx} \\ E_{ty} \end{pmatrix} = \begin{pmatrix} z_p\cos^2\alpha\cos\frac{\omega t}{2} - z_s\sin\alpha\cos\alpha\sin\frac{\omega t}{2} \\ z_p\sin\alpha\cos\alpha\cos\frac{\omega t}{2} - z_s\sin^2\alpha\sin\frac{\omega t}{2} \end{pmatrix}, \quad (1)$$

where S is the Jones matrix for the test medium, and z_p and z_s are the associated parameters of the p- and s-polarizations. If the refractive indices of the glass substrate, air, and the metallic mirror are n_1, n_2, and n_3, respectively, then they can be expressed as [9]

$$z_p = \frac{r_{12,p} + r_{23,p}\exp(i\beta)}{1 + r_{12,p}r_{23,p}\exp(i\beta)}, \quad (2a)$$

and

$$z_s = \frac{r_{12,s} + r_{23,s}\exp(i\beta)}{1 + r_{12,s}r_{23,s}\exp(i\beta)}, \quad (2b)$$

where r_{lm} is the amplitude reflection coefficient at the interface as the light beam from medium l is incident at θ_l on medium m, in which the light beam is refracted at θ_m. According to Fresnel's equation, we have [9]

$$r_{lm,p} = \frac{n_l\cos\theta_m - n_m\cos\theta_l}{n_l\cos\theta_m + n_m\cos\theta_l}, \quad (3a)$$

and

$$r_{lm,s} = \frac{n_l\cos\theta_l - n_m\cos\theta_m}{n_l\cos\theta_l + n_m\cos\theta_m}. \tag{3b}$$

In addition, the phase β comes from the optical path-length difference between two neighbor reflected beams and it can be written as

$$\beta = \frac{4\pi n_2 d\cos(\theta_2)}{\lambda}, \tag{3c}$$

where λ is the wavelength of the light beam, and d is the thickness of the thin air gap between the glass plate and the mirror. Consequently, the intensity of the test beam received by the photodetector D can be derived as [10]

$$I_t = |E_t|^2 = \left(E_{tx}^2 + E_{ty}^2\right)^{1/2} = I_0[1 + \gamma\cos(\omega t + \phi)], \tag{4}$$

where I_0, γ, and ϕ are the mean intensity, the visibility, and the phase of the interference signal, respectively. They can be expressed as

$$I_0 = \frac{1}{2}\left(|z_p|^2\cos^2\alpha + |z_s|^2\sin^2\alpha\right), \tag{5a}$$

$$\gamma = \frac{\sqrt{\frac{1}{4}\left(|z_p|^2\cos^2\alpha - |z_s|^2\sin^2\alpha\right)^2 + \left(z_p z_s^* + z_s z_p^*\right)^2\sin^2\alpha\cos^2\alpha}}{I_0}, \tag{5b}$$

and

$$\phi = \tan^{-1}\left[\frac{(z_p z_s^* + z_s z_p^*)\sin 2\alpha}{|z_p|^2\cos^2\alpha - |z_s|^2\sin^2\alpha}\right], \tag{5c}$$

where z_p^* and z_s^* are the conjugates of z_p and z_s, respectively.

On the other hand, the modulated electronic signal of the circular heterodyne light source is filtered and used as the reference signal. It has the form

$$I_r = \frac{1}{2}[1 + \cos(\omega t)]. \tag{6}$$

Both of these two sinusoidal signals I_t and I_r are sent to a phase meter PM and ϕ can be measured accurately. From Eqs. (2a) (2b), (3a) (3b) and (5a) (5b) (5c), it is obvious that the phase difference ϕ is a function of n_2, d, i_0, and α under the experimental conditions in which n_1 and n_3 are specified. It can be experimentally measured for each given α under a fixed incident angle i_0. To evaluate the values of n_2 and d, we required two different phase differences ϕ_1 and ϕ_2 that correspond to two azimuth angles, α_1 and α_2. Hence, a set of simultaneous equations

$$\phi_i = f(n_2, d, \alpha_i) \quad (i = 1, 2) \tag{7a}$$

is obtained. If these two equations are solved, the refractive index n_2 and the thickness d of the air gap can be estimated,

simultaneously. For absorbing materials n_2 should be changed to $n_2 + ik_2$. To solve this parameter k_2, an additional phase difference ϕ_3 under the azimuth angle α_3 should be measured. Similarly, the following set of simultaneous equations

$$\phi_i = f(n_2, k_2, d, \alpha_i) \quad (i = 1, 2, 3) \tag{7b}$$

is solved, then n_2, k_2 and d can be estimated. Therefore, it is obvious that this method is also suitable for measuring absorbing materials.

3. Experiments and results

To show the feasibility of this method, we designed a substitute structure to simulate the dynamic behavior of the thin film growth or etching. This structure was composed of a glass plate (BK7) and a metallic (Au) mirror mounted on a high precision motorized-mount (model: PZ/91, Burleigh Instruments). The flatness and parallelism of their surfaces are better than $\lambda/20$ and 20 arc sec. To avoid optical contacting and get an easy optical alignment for parallelism of the glass plate and the mirror, the glass plate was separated from the mirror by a small air gap with 2 mm. The change of the air spacing thickness mimicked the thickness variation in the thin film growth or etching process as the mirror was moved toward or away from the glass plate. Both of them were mounted on a precision rotation stage with angular resolution 0.005° (model: PS-θ-90, Chou Precision Industrial Company Ltd.). A circular polarized heterodyne light source consisting of a linearly polarized He-Ne laser at 632.8 nm, an electro-optic modulator EO (model: 4001, New Focus, Inc.), and a quarter-wave plate Q was used as shown in Fig. 1(b). The fast axes of EO and Q were located at 45° and 0° to the x-axis, respectively. The frequency difference between the left- and right-circular polarizations was 1 kHz. The conditions $i_0 = 80°$, $\alpha_1 = 40°$ and $\alpha_2 = 45°$ were chosen. The corresponding phase differences were measured by a home-made phase meter with an angular resolution 0.001°, and the measured results are shown in Table 1. The estimated results and the reference data of the optical constants of air are also shown in Table 1, and the estimated results of the simulated-thickness variations of the thin film growth and the associated PZT displacements versus the phase difference ϕ are shown in Fig. 3. Here the displacement of the PZT was obtained with the experimental characteristic curve of the displacement

Table 1
Average value of the measured data, estimated result n and the reference data

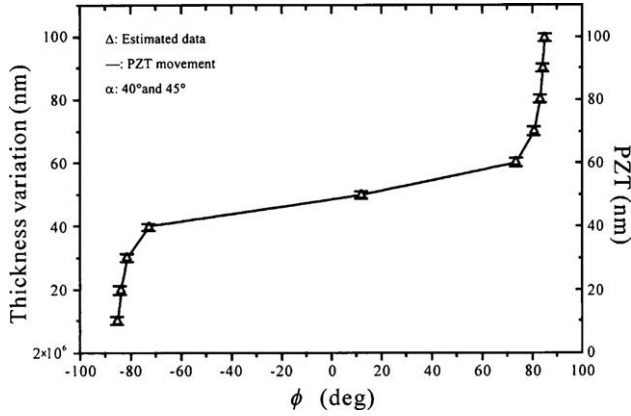| α (°)	$\phi_{Ave.}$ (°)	Standard deviation (°)	n_2 (ave.)	n_2 (Ref.) [10]
40	−79.869	+0.948	1.00038	1.000293
45	−84.836	+0.609		

Fig. 3. Estimated results of simulated thickness variations and PZT displacement versus phase difference ϕ. Note: The symbols Δ and I represent the average value of 50 measured data points and the associated standard deviation, respectively.

versus the applied voltage [11]. From Table 1 and Fig. 3, it is clear that they show good correspondence.

4. Discussion

To estimate the errors in n_2 and d, we can differentiate Eq. (5c) with respect to n_2 and d. It can be expressed as:

$$\Delta\phi_x = \frac{\partial\phi(n_2, d, \alpha_x)}{\partial n_2}|\Delta n_2|$$
$$+ \frac{\partial\phi(n_2, d, \alpha_x)}{\partial d}|\Delta d|, \quad \text{(for } x = 1, 2) \tag{8}$$

where $|\Delta n_2|$ and $|\Delta d|$ are the errors in n_2 and d, respectively. They can be expressed as

$$|\Delta n_2| = \left|\frac{B_2\Delta\phi_1 - B_1\Delta\phi_2}{A_1B_2 - A_2B_1}\right|, \tag{9a}$$

$$|\Delta d| = \left|\frac{A_2\Delta\phi_1 - A_1\Delta\phi_2}{A_2B_1 - A_1B_2}\right|, \tag{9b}$$

and

$$A_x = \left|\frac{\partial\phi(n_2, d, \alpha_x)}{\partial n_2}\right|,$$
$$B_x = \left|\frac{\partial\phi(n_2, d, \alpha_x)}{\partial d}\right|, \quad \text{(for } x = 1, 2) \tag{9c}$$

where $\Delta\phi_1$ and $\Delta\phi_2$ are the errors in phase differences ϕ_1 and ϕ_2, respectively. By taking into account the angular resolution of the phase-meter, the second-harmonic error and the polarization-mixing errors, $\Delta\phi_1 = \Delta\phi_2 \approx 0.03°$ can be estimated in our experiments [12]. Substituting these data and experimental conditions into Eqs. (8) (9a) (9b) (9c), the corresponding errors in n_2 and d are $|\Delta n_2| = 6.9 \times 10^{-5}$ and $|\Delta d| = 9 \times 10^{-2}$ nm, respectively. If the experimental standard deviation is taken into account, then $|\Delta n_2|$ and $|\Delta d|$ will be 7.1×10^{-4} and

0.87 nm, respectively. It is obvious that they are similar to the estimated corresponding errors.

As there are two unknowns (n_2 and d), we need at least two equations to solve them. These can be obtained by measuring ϕ at two different azimuth angles of the analyzer as described above. Hence this method is easier to operate in the optical setup by changing the azimuth angles of an analyzer instead of changing the incident angles in other methods [1,4]. Referring to its convenience, it is similar to the in situ ellipsometry, in which two parameters ψ and Δ can be obtained at a single incident angle. The intensity variations are measured in the in situ ellipsometry, and the phase variations are measured in this method. To our knowledge there are no published works on the results of the thin film growth measurement by circular heterodyne interferometry. In Fig. 3, it is obvious that resolution is not good enough when the thickness variation is larger than 70 nm or lower than 40 nm. Because the resolution depends both on the azimuth angle and incident angle, we can optimize the experiment conditions of the azimuth angle and incident angle with scanning α and i_0. then the high resolution can be achieved. Moreover, our method is feasible and useful in in situ monitoring and controlling the thickness of the thin film growth in the MBE system, although we demonstrate a simulated measurement configuration here. Based on Eqs. (2a) (2b), (3a) (3b) (3c), and (5c), the relation curves of phase difference versus the thickness of SiO_2 thin film deposited on an Si substrate under single azimuth angle ($\alpha = 45°$) and three different incident angles are shown in Fig. 4. Their slopes are almost 1.462 (°/nm), 1.456 (°/nm), and 0.797 (°/nm) for curves A, B, and C, respectively. Under our experimental conditions, their resolutions are roughly 0.021, 0.021, and 0.038 nm, respectively. In principle, this method could be applied to obtain the measurement in small thickness variation. From the relationship shown in Fig. 4, it is also suggested that the applicable range for this method is for thickness variation
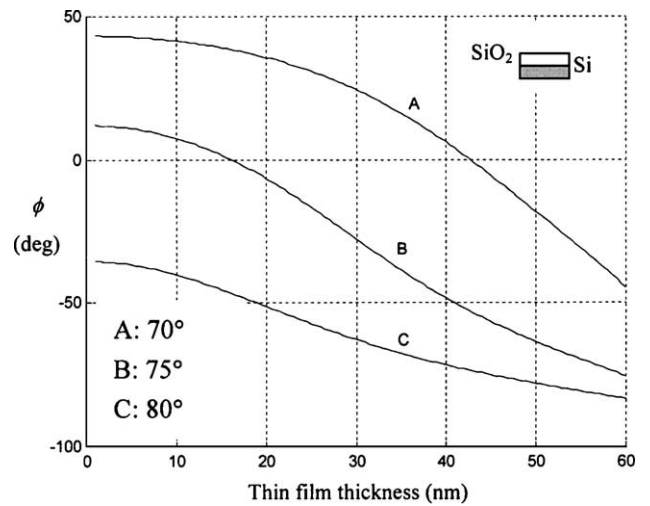

Fig. 4. Phase difference versus thin film thickness under three different incident angles: 70°, 75°, and 80°.

less than 60 nm with optimal experimental conditions. For example, the typical thickness of the SiO_x layer used in a bipolar transistor serving as the base is about in the range of a few nanometers [13]. For better resolution in determining the thickness of the SiO_x layer, the incident angle could be chosen at 75° according to the theoretical data as shown in Fig. 4. Hence, this method can be applied to measure the thickness variation under the thin film growth process even for ultra-thin film growth. However, it will be more complicated to apply our method into the real MBE system and some critical conditions should be contemplated, such as the scattering effect coming from the test beam interacting with the molecule in the MBE chamber, anisotropy signal coming from the thin film growth process, optical-elastic effect of the glass plate on the MBE windows, and wafer wobbling effect during the layer deposition. If the low birefringence glass is used as MBE windows, then its optical-elastic effect can be neglected [2]. Hence, further experiments are in progress, such as the combination of MBE system and circular heterodyne interferometry, and improvement in calculation as the scattering effect, wafer wobbling effect, and anisotropic effect are in consideration.

For spectral optical constants measurement, a broadband light source and interference filters can be used to replace the laser light source. The half-wave voltage of the modulated electronic signal applied to the electro-optic modulator EO should be changed accordingly as the wavelength varies. Then the broad-spectrum optical properties of the thin film can be achieved.

5. Conclusion

In this paper, we present an alternative method that can measure the thickness and refractive index of the thin film as the growth process is ongoing. Based on the common-path optical configuration, this method is free from environmental vibration and thus high stability can be achieved. From the theoretical prediction, the resolution of the thickness of the thin film is about 0.021 and 0.038 nm for different simulation case. In addition, this method also has many merits, such as simple setup, easy operation, and measurement of multi-parameters with a single configuration.

References

[1] J.J. Chen, J.D. Lin, L.J. Sheu, Thin Solid Films 354 (1999) 176.
[2] N.K. Zayer, R. Greef, K. Rogers, A.J.C. Grellier, C.N. Pannell, Thin Solid Films 352 (1999) 179.
[3] N. Fujimura, T. Nishihara, S. Goto, J. Xu, T. Ito, J. Cryst. Growth 130 (1993) 269.
[4] Y.G. Mo, R.O. Dillon, P.G. Snyder, J. Vac. Sci. Technol., A 17 (1999) 170.
[5] B.P. Singh, Appl. Surf. Sci. 150 (1999) 95.
[6] G.N. Maragas, C.H. Kuo, S. Anand, R. Droopad, G.R.L. Sohie, T. Levola, J. Vac. Sci. Technol., A 13 (1995) 727.
[7] M. Henini, III–Vs Rev. 13 (2000) 18.
[8] C.C. Hsu, D.C. Su, Appl. Opt. 41 (2002) 3936.
[9] M. Born, E. Wolf, Principles of Optics, Pergamon, Oxford, UK, 1980, Chapter 1.
[10] E. Hecht, Optics, Addison-Wesley, USA, 1990, p. 334.
[11] M.H. Chiu, J.Y. Lee, D.C. Su, J. Opt. 29 (1998) 349.
[12] M.H. Chiu, J.Y. Lee, D.C. Su, Appl. Opt. 38 (1999) 4047.
[13] P. Petrik, T. Lohner, M. Fried, J. Gyulai, U. Boell, R. Berger, W. Lehnert, J. Appl. Phys. 92 (2002) 2374.